Accelerated Aging in Electrolytic Capacitors for Prognostics

José R. Celaya, PhD, SGT Inc.

Chetan Kulkarni, Vanderbilt University

Sankalita Saha, PhD, MCT

Gautam Biswas, PhD, Vanderbilt University

Kai Goebel, PhD, NASA Ames Research Center

SUMMARY AND CONCLUSIONS

The focus of this work is the analysis of different degradation phenomena based on thermal overstress and electrical overstress accelerated aging systems and the use of accelerated aging techniques for prognostics algorithm development. Results on thermal overstress and electrical overstress experiments are presented. In addition, preliminary results toward the development of physics-based degradation models are presented focusing on the electrolyte evaporation failure mechanism. An empirical degradation model based on percentage capacitance loss under electrical overstress is presented and used in: (i) a Bayesian-based implementation of model-based prognostics using a discrete Kalman filter for health state estimation, and (ii) a dynamic system representation of the degradation model for forecasting and remaining useful life (RUL) estimation. A leave-one-out validation methodology is used to assess the validity of the methodology under the small sample size constrain.

The results observed on the RUL estimation are consistent through the validation tests comparing relative accuracy and prediction error. It has been observed that the inaccuracy of the model to represent the change in degradation behavior observed at the end of the test data is consistent throughout the validation tests, indicating the need of a more detailed degradation model or the use of an algorithm that could estimate model parameters on-line. Based on the observed degradation process under different stress intensity with rest periods, the need for more sophisticated degradation models is further supported. The current degradation model does not represent the capacitance recovery over rest periods following an accelerated aging stress period.

1 INTRODUCTION

Electrolytic capacitors have become critical components in electronics systems in aeronautics and other domains. This type of capacitors is known for its low reliability and frequent breakdown on critical systems like power supplies of avionics equipment [1]. The field of prognostics for electronics components is concerned with the prediction of remaining useful life of components and systems. In particular, it focuses on condition-based health assessment by estimating the current state of health. Furthermore, it leverages the knowledge of the device physics and degradation physics to predict remaining useful life as a function of current state of health and anticipated operational and environmental conditions. The development of prognostics methods for electronics present several challenges due to great variety of components used in a system, a continuous development of new electronics technologies, and a general lack of understanding of how electronics fail. Traditional reliability techniques in electronics tend to focus on understanding the time to failure for a batch of components of the same type. Recently, there has been a push to understand, in more depth, how a fault progresses as a function of usage, namely, loading and environmental conditions.

The motivation of this work comes from avionics systems on-board autonomous aircraft. These systems perform critical functions and incipient failures are likely to escalate to an in-flight malfunction [2]. Hence, a systematic analysis of degradation and fault conditions is very important for analysis of aircraft safety and to avoid catastrophic failures during flight. DC-DC converters are studied in this context as a system sourcing power to the global positioning systems and navigation subsystems given that those faults in the DC-DC converters propagate to the navigation systems affecting overall operation. Electrolytic capacitors used as output filters in DC-DC converters cause performance degradation and failures resulting in a ripple voltage surge at the power supply output leading to navigation errors [1].

The prognostics methodology presented here is based on results from an accelerated life test on real electrolytic capacitors as described in Figure 1. This test is applied to commercial-off-the-shelf capacitors in order to observe the degradation process and identify precursors of failure. Electro-impedance spectroscopy is used periodically during the test to characterize the frequency response of the capacitor impedance and monitor performance degradation. A degradation model structure is suggested based on the observed degradation curves. The model parameters are estimated using nonlinear least-squares regression. A Bayesian framework is employed to estimate the state of health based on measurement updates.
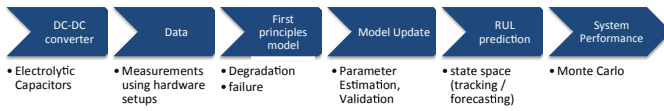
Figure 1. Model-based prognostics methodology for electrolytic capacitor.

2 ACCELERATED LIFE EXPERIMENTS

Accelerated life test methods are used in electronics prognostics research as a way to assess the effects of the degradation process through time in a reduced timescale. It allows for the identification and study of different failure mechanisms and their relationships with different observable signals and parameters. This is accomplished by recording several signals through the degradation process, and generating run-to-failure data for experiments with different stress levels.

Electrolytic capacitors of 2200µF, with a maximum rated voltage of 10V, maximum current rating of 1A and maximum operating temperature of 105°C were used for the study. These are the recommended capacitors by the manufacturer for DC-DC converters used in our previous work. The electrolytic capacitors under test were characterized before the start of the experiment. In particular, the equivalent series resistance (ESR) and capacitance values were measured using an SP-150 Biologic electro-impedance spectroscopy instrument. The average measured initial ESR value for the test group was 0.056mΩ and average capacitance was 2123µF.

2.1 Electrical overstress accelerated aging (EOS)

The objective of this experiment is studying the effects of voltage stress in capacitors. The capacitors were subjected to voltage stress through an external supply source using custom hardware. The measured frequency response of the capacitor's impedance is used to estimate ESR and capacitance, and assess performance degradation.

The capacitors are subjected to different stress levels during the aging test. Figure 2 shows a plot of the decrease in the value of the capacitance for all six capacitors under EOS. In the first condition (a), capacitors are charged and discharged with a square waveform of 200 mHz, 12V amplitude with a load of 100 ohms up to 200 hours of aging time. From 200 to 3000 hours (b), the capacitors were at rest, after which, they were subjected to (c), 12V EOS for the next 100 hours. From 3100 hours up to 5000 hours (d), the capacitors were charged and discharged with a square waveform of 200 mHz, (-6 to 6) V with a load of 100 ohms. In the last phase (e), the capacitors were again subjected to 12V EOS condition. All the capacitors under test are subjected to similar environment conditions, their ESR and capacitance values are monitored periodically. The tests are conducted at room temperature. For further details regarding the aging experiment set up refer to [3, 4].

As per the standards [5], a capacitor is considered failed if under electrical operation, its ESR increases by 280-300% of its initial value or the capacitance decreases by 20% below its pristine condition value. From the plots we observe that during the initial period when capacitors were subjected to 12V EOS, a higher degradation rate was observed as compared to the next 4500 hours of operation where the charging/discharging took place below the rated voltage. At the end of 5000 hours when the capacitors were again subjected to 12V EOS there was a rapid decrease observed in the capacitance value which in hypothesis, is a sudden breakdown.

The observed degradation profile for EOS aging supports the notion that, at higher the intensity level, namely the amplitude of the charge/discharge signal, results in higher degradation rate. This is mainly observed by comparing segments (c) and (d) in the aging profile of Figure 2. In addition, it supports the notion that a degradation rate for a particular stress level could be different at different stages of the lifetime of the capacitor. This is supported by observing segments (a) and (e). Finally, the most important finding of this work in the presence of self-recovery of the capacitor's performance as observed in segment (b). This has implications in the development of degradation models for prognostics. The degradation model presented in [4, 6] and later is Section 3.1, does not include this behavior and should be updated in future work. The self-recovery behavior is believed to represent very slow internal dynamics that do not reach steady state at the time of the characterization of devices, which happens right after the EOS is applied for a long period.
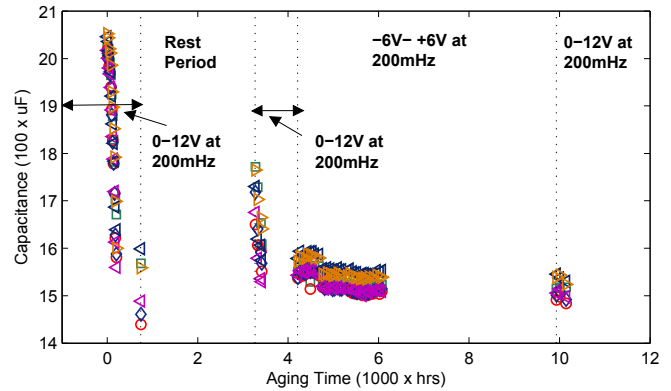

Figure 2. Degradation of capacitor performance Capacitance decreases, as function of aging time.

2.2 Thermal overstress accelerated aging

In this aging experiment we emulated conditions similar to high temperature storage, where capacitors are placed in a controlled chamber and the temperature is raised above their rated specification [4, 7]. The chamber temperature was gradually increased in steps of 25°C until the pre-determined temperature limit was reached. The capacitors were allowed to settle at a set temperature for about 15 min and then the next step increase was applied; this process continued until the desired aging temperature is reached. This procedure was followed in order to avoid thermal shocks due to sudden increase/decrease in temperature. For this experiment, six capacitors were subjected to a constant temperature of 125°C with no temperature variation. At the end of specific time interval the temperature was lowered in steps of 25°C till the

required room temperature was reached.

As the devices degrade we observe a considerable decrease in the capacitance and less change in the ESR. Under thermal stress it is observed that the degradation in the capacitors is primarily due to decrease in the capacitance [8, 9]. In this experiment the failure precursor is linked to the decrease in the capacitance value. As per the standards MIL-C-62F14 [5] a capacitor is considered failed if under storage condition and high thermal stress its capacitance decreases by 10% or more below its pristine condition value. Figure 3 shows the plots for all the six capacitors under test. The decrease in capacitance is plotted as a function of aging time.

It was observed that, as the temperature increases, the electrolyte inside the capacitors evaporates and from equations (2) and (3) (presented in Section 3.2) the decrease in the capacitance is directly linked to the decrease in the effective oxide area (A_0) of the capacitor. This decrease in the oxide area is, in turn, directly related to the rate of evaporation of the electrolyte given by equation (2). At ~2200 hours of aging, we observe a linear decrease in capacitance as predicted by the physics of failure model. As we continue beyond this time period, at around 2250-2400 hours we observe a step change in the capacitance indicating a sudden breakdown.
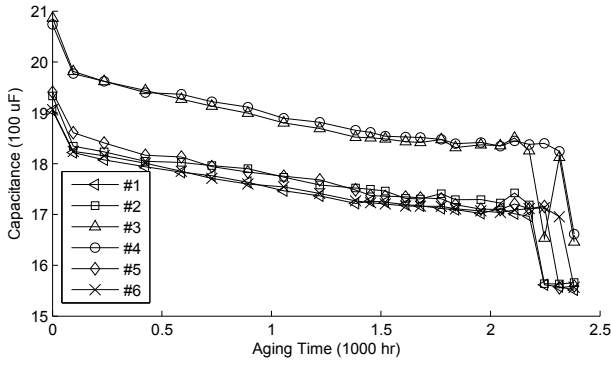

Figure 3. Thermal overstress aging results.

3 MODELING OF THE DEGRADATION PROCESS

The literature on capacitor degradation shows a direct relationship between electrolyte decrease and increase in the ESR of the capacitor [10]. ESR increase implies greater dissipation, and, therefore, a slow decrease in the average output voltage at the capacitor leads. Another mechanism occurring simultaneously is the increase in internal pressure due to an increased rate of chemical reactions, which are attributed to the internal temperature increase in the capacitor. This information relating failure mechanism to performance parameters is used to build degradation models for prognostics algorithm development. In this context, a degradation model relates usage time to a change in a performance parameter from pristine condition through failure. An empirical model based on the EOS experiments described in Section 3.1 is presented, as well as initial developments of a physics-based degradation model based on the electrolyte evaporation failure mechanism.

3.1 Empirical degradation model under electrical overstress

An empirical model can be constructed by observing the degradation behavior on accelerated aging tests. The percentage loss in capacitance is used as a precursor of failure variable and it is used to build a model of the degradation process (Figure 4). The behavior presented in Figure 4 corresponds to the first segment of aging in Figure 2. This model, originally introduced in [4, 6], relates aging time to the percentage loss in capacitance and has the following form,

$$C_k = e^{\alpha t_k} + \beta, \tag{1}$$

where α and β are constants that will be estimated from the experimental data of accelerated aging experiments. In order to estimate the model parameters, five capacitors are used for estimation and the remaining capacitor is used to test the prognostics algorithm. A nonlinear least-squares regression algorithm is used to estimate the model parameters. The estimated parameters are $\hat{\alpha}$ and $\hat{\beta}$ presented in Table 1 for five different test scenarios.
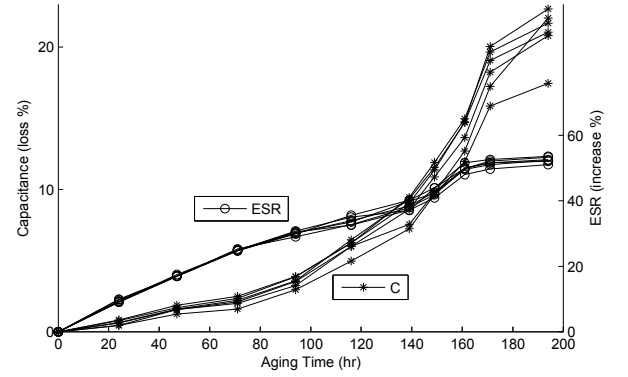

Figure 4. Percentage degrease in capacitance and percentage increase in ESR for EOS data from Figure 2.

Table 1. Empirical model parameter estimation results for five test cases. The optimal parameter is presented along the 95% confidence interval. The residuals are modeled as a normally distributed random variable with zero mean and variance σ_v^2.

Test	Test Cap.	Training Caps.	$\hat{\alpha}$ 95% CI	$\hat{\beta}$ 95% CI	$\hat{\sigma}_v^2$
T_2	2	1, 3-6	**0.0162** (0.0160, 0.0164)	**-0.8398** (-1.1373, -0.5423)	1.8778
T_3	3	1, 2, 4-6	**0.0162** (0.0160, 0.0164)	**-0.8287** (-1.1211, -0.5363)	1.9654
T_4	4	1-3, 5, 6	**0.0161** (0.0159, 0.0162)	**-0.8217** (-1.1125, -0.5308)	1.8860
T_5	5	1-4, 6	**0.0162** (0.0161, 0.0164)	**-0.7847** (-1.1134, -0.4560)	2.1041
T_6	6	1-5	**0.0169** (0.0167, 0.0170	**-1.0049** (-1.2646, -0.7453)	2.9812

These scenarios correspond to the leave-one-out validation process. It is observed, from the estimated values

and their corresponding confidence intervals, that the model structure does a reasonable job describing the behavior of the observed degradation process.

3.2 Physics-based modeling under thermal stress

The structure of electrolytic capacitors is considered as a long strip line structure, which is cylindrically wound and packed in a case. Figure 5 shows the anode and cathode, the dielectric oxide layers, and electrolyte interconnecting layer [11]. The total lumped capacitance of the structure is given by

$$C(t) = \frac{\epsilon_R \epsilon_0 A_0(t)}{t_0}, \qquad (2)$$

where ϵ_R is the relative dielectric constant, ϵ_0 is the permittivity of free space and t_0: oxide thickness. The capacitance value is directly proportional to the oxide layer area and inversely proportional to the oxide thickness.

Increase in the core temperature of the capacitor due to electrical or thermal overstress accelerates the rate of electrolyte evaporation leading to degradation of the capacitance [9, 11]. The following models relate to degradation in performance due to electrolyte evaporation.

The depletion in the electrolyte volume and thus the effective surface area is given by

$$V(t) = V_0 - A_0(t)j_{eo}t, \qquad (3)$$

where $V(t)$ is the dispersion volume at time t, V_0 is the initial dispersion volume, $A_0(t)$ is the oxide surface area of evaporation and j_{eo} is the evaporation rate. Details of the derivation of this equation can be found in [11, 12]. Equation (3) gives us the decrease in the electrolyte volume due to evaporation, which results in a decrease in C and an increase in ESR [13, 14].

For a healthy capacitor operating nominally, leakage current is not significant, but it begins to increase as the oxide layer degrades, which can be attributed to crystal defects that occur due to electrolyte evaporation under thermal overstress conditions [9, 14]. This can be further explained by the decrease in electrolyte resistance (R_E) as derived in equation (4). Therefore, decrease in R_E increases the leakage current through the capacitor.

The total lumped electrolyte resistance for a rolled configuration is

$$R_E(t) = \frac{\rho_E t_0 P_E(t)}{2A_0(t)}, \qquad (4)$$

where ρ_E is the electrolyte resistivity and $P_E(t)$ is the correlation factor related to electrolyte spacer porosity and average liquid pathway. With decrease in the electrolyte due to high temperature, the average liquid path length is reduced, which decreases P_E directly. The decrease in P_E reduces R_E as the electrolyte evaporates.

In summary, the degradation in the capacitor under thermal stress can be linked to two parameters: A_0 and P_E, which directly affect the capacitance and leakage current, respectively.
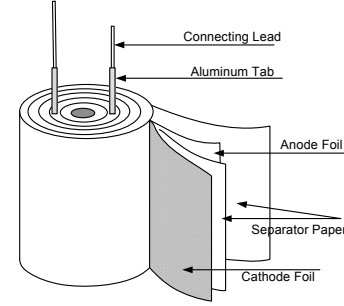

Figure 5. Structure of an electrolytic capacitor.

4 PROGNOSTICS ALGORITHM DEVELOPMENT

The empirical degradation model in Section 3.1 is used as part of a Bayesian tracking framework to be implemented using the Kalman filter technique. This method requires a state-space dynamic model relating the degradation level at time t_k to the degradation level at time t_{k-1}.

The following system structure is used in the implementation of the filtering and prediction using the Kalman filter. This is a discrete-time state-space structure for a dynamic system given by the state equation $C_k = A_k C_{k-1} + B_k u + v$ and the measurement equation $y_k = hC_k + w$. The degradation model in equation (1) is expressed in the structure of the state equation resulting in $A_k = 1 + \Delta_t$, $B_k = -\alpha\beta\Delta_k$ and $u = 1$. In this model C_k is the state variable and it represents the percentage loss in capacitance. Since the system measurements are percentage loss in capacitance as well, the output equation is given by $y_k = hC_k$, where $h = 1$. Furthermore, v and w are normal random variables with zero mean, and variances Q and R respectively. The model noise variance Q was estimated from the model regression residuals. The residuals have a mean very close to zero and a variance for all test cases are presented in Table 1. This variance was used for the model noise in the Kalman filter implementation. The measurement noise variance R is also required in the filter implementation. This variance was computed from the direct measurements of the capacitance with the electro-impedance spectroscopy equipment, the observed variance is 4.9×10^{-7} (F^2).

The use of the Kalman filter as a forecasting algorithm requires the evolution of the state without updating the error covariance matrix and the posterior of the state vector. The n step ahead forecasting equation for the Kalman filter is $\hat{C}_{l+n} = A^n C_l + \sum_{i=0}^{n-1} A^i B$. The last update is done at the time of the last measurement t_l. The failure threshold is considered to be a crisp value of 20% decrease in capacitance. End of life (EOL) is defined as the time at which the forecasted percentage capacity loss trajectory crosses the EOL threshold. This methodology was originally introduced in detail [4, 6].

Figure 6 presents the capacitance loss estimation and EOL prediction at different points during the aging time. Predictions are made at points in which measurements are available. Only predictions at $t_p = [116,139,149,161]$ for

test case T_6 are shown due to space limitations. The complete estimation results are presented in Table 2. It can be observed that the predictions become more accurate as the prediction is made closer to the actual EOL. This is possible because of the estimation process has more information to update the estimates as it gets closer to EOL.
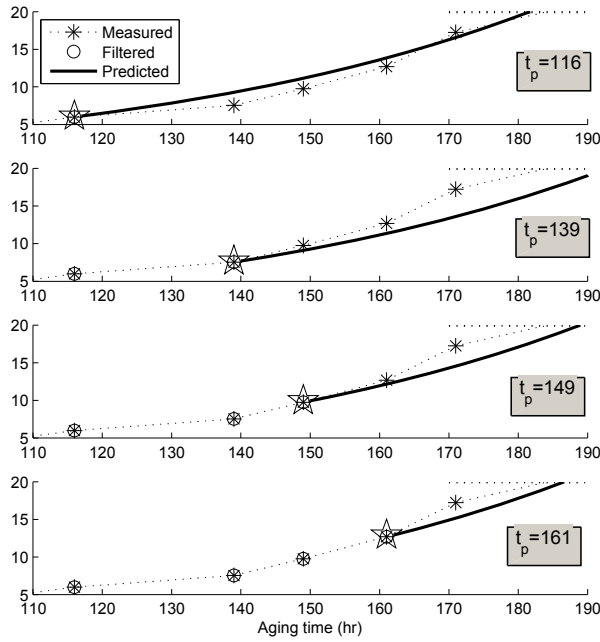

Figure 6. Health state estimation and forecasting of capacitance loss (%) at different times t_p during the aging time; t_p=[116, 139, 149, 161].

Table 2. RUL estimation results for the five test cases (Table 1) at different prediction times (all values are in hours).

t_p	RUL^*	RUL'_{T2}	RUL'_{T3}	RUL'_{T4}	RUL'_{T5}	RUL'_{T6}
24	151.04	158.84	164.88	158.76	167.76	159.89
47	128.04	131.32	134.08	128.35	135.32	125.91
71	104.04	117.01	119.88	115.37	122.63	116.41
94	81.04	92.69	96.64	93.09	97.60	95.42
116	59.04	67.28	65.39	67.77	69.50	65.71
139	36.04	44.01	44.72	46.88	49.40	53.75
149	26.04	30.67	32.41	33.55	35.92	39.95
161	14.04	17.23	18.28	18.20	22.64	25.60
171	4.04	1.07	2.89	N/A	5.52	8.45

The remaining useful life predictions results for all test cases support the conclusions previously drawn for a single case (T_6) in [4, 6]. The proposed empirical degradation model and the Kalman filter-based method is able to estimate RUL with reasonable performance given that the degradation model parameters are fixed and not updated through time. Under the leave one out validation presented here, the algorithm is able to provide with coherent RUL estimates under the 5 established test scenarios. Table 3 shows performance based on the relative accuracy (RA) metric in equation (5). These metrics allows for an assessment of the percentage accuracy

relative to the ground-truth value. RA values of 100 represent perfect accuracy. The RA is presented for all the test cases for different prediction times. The last column of the Table 3 represents the median RA of all the test cases for a particular prediction time. It is observed that the RA values decrease considerably for $t_p = 171$. This is consistent with previous observations indicating that the algorithm with a fixed-parameter model is not able to cope with the sudden jump in exponential behavior present around the 171 hour. This is a limitation that could be overcome by either an enhanced degradation model or a an online estimation of degradation model parameters using a more sophisticated Bayesian tracking method like extended Kalman filter or particle filter.

$$RA \stackrel{\text{def}}{=} 100\left(1 - \frac{|RUL^* - RUL'|}{RUL^*}\right) \qquad (5)$$

Table 3. Relative accuracy metric for the RUL estimation.

t_p	RA_{T2}	RA_{T3}	RA_{T4}	RA_{T5}	RA_{T6}	$\widetilde{RA}$
24	94.8	95.5	91.9	96.9	99.7	**95.5**
47	97.4	99.3	96.4	96.7	91.7	**96.7**
71	87.5	91.9	84.5	94.1	97.1	**91.9**
94	85.6	90	78.9	94.8	94.2	**90**
116	86	99.1	76.5	98.0	96.2	**96.2**
139	77.8	95.8	53.1	96.7	81.1	**81.1**
149	82.1	98.4	46.9	94.8	86.6	**86.6**
161	77.2	87.3	16.6	87.5	89.8	**87.3**
171	26.6	26.4	N/A	34.8	63.7	**30.7**

REFERENCES

1. Kulkarni, C., G. Biswas, R. Bharadwaj, and K. Kim, "Effects of Degradation in DC-DC Converters on Avionics Systems: A Model Based Approach". *Machinery Failure Prevention Technology Conference, MFPT*, 2010.
2. Kulkarni, C., G. Biswas, and X. Koutsoukos, "A prognosis case study for electrolytic capacitor degradation in DC-DC converters". *Annual Conference of the Prognostics and Health Management Soceity*, 2009.
3. Kulkarni, C., G. Biswas, X. Koutsoukos, J. Celaya, and K. Goebel. "Integrated diagnostic/prognostic experimental setup for capacitor degradation and health monitoring". in *IEEE AUTOTESTCON*. 2010.
4. Celaya, J., C. Kulkarni, G. Biswas, and K. Goebel. "Towards Prognostics of Electrolytic Capacitors". in *AIAA Infotech@Aerospace Conference*. 2011. St. Louis, MO.
5. MIL-C-62F, "General Specification For Capacitors, Fixed, Electrolytic", 2008.
6. Celaya, J., C. Kulkarni, G. Biswas, S. Saha, and K. Goebel. "A Model-based Prognostics Methodology for Electrolytic Capacitors Based on Electrical Overstress Accelerated Aging". in *Annual Conference of the Prognostics and Health Management Society*. 2011. Montreal, Canada: PHM Society.
7. IEC, "Environmental testing. Part 1: General and guidance (IEC 60068-1 ed6.0)", 2007.

8. Biologic, "Application note 14-Zfit and equivalent electrical circuits", 2010.
9. IEC, "60384-4-1 Fixed capacitors for use in electronic equipment", 2007-03.
10. Kulkarni, C., G. Biswas, X. Koutsoukos, K. Goebel, and J. Celaya. "Physics of Failure Models for Capacitor Degradation in DC-DC Converters". in *The Maintenance and Reliability Conference, MARCON*. 2010.
11. Rusdi, M., Y. Moroi, H. Nakahara, and O. Shibata, "Evaporation from Water, Ethylene Glycol Liquid Mixture". *Langmuir*, 2005. **21**(16): p. 7308-7310.
12. Kulkarni, C.S., G. Biswas, J. Celaya, and K. Goebel. "Prognostic Techniques for Capacitor Degradation and Health Monitoring". in *8th International Workshop on Structural Health Monitoring, IWSHM*. 2011.
13. Bengt, A., "Electrolytic Capacitors Theory and Applications", 1995, RIFA Electrolytic Capacitors: Sweden.
14. Roederstein, V., "Aluminum Capacitors- General Information (Document # 25001)", 2007.

BIOGRAPHIES

José R. Celaya, PhD.
NASA Ames Research Center (SGT Inc.)
Prognostics Center of Excellence
MS 269-4
Moffett Field, CA 94035, USA

email: jose.r.celaya@nasa.gov

José R. Celaya is a Research Scientist with SGT Inc. at the Prognostics Center of Excellence, NASA Ames Research Center. He received a PhD degree in Decision Sciences and Engineering Systems in 2008, a M. E. degree in Operations Research and Statistics in 2008, a M. S. degree in Electrical Engineering in 2003, all from Rensselaer Polytechnic Institute, Troy New York; and a B. S. in Cybernetics Engineering in 2001 from CETYS University, México.

Chetan Kulkarni
ISIS, Vanderbilt University
1025 16th Avenue
Nashville, TN, 37212, USA

email: chetan.kulkarni@vanderbilt.edu

Chetan S Kulkarni is a Research Assistant at ISIS, Vanderbilt University. He received the M.S. degree in EECS from Vanderbilt University, Nashville, TN, in 2009, where he is currently a PhD student.

Sankalita Saha, PhD
NASA Ames Research Center (MCT)
Prognostics Center of Excellence
MS 269-4
Moffett Field, CA 94035, USA

email: sankalita.saha@nasa.gov

Sankalita Saha is a Research Scientist with Mission Critical Technologies at the Prognostics Center of Excellence, NASA Ames Research Center. She received the M.S. and PhD degrees in Electrical Engineering from University of Maryland, College Park in 2007. Prior to that she obtained her B.Tech (Bachelor of Technology) degree in Electronics and Electrical Communications Engineering from the Indian Institute of Technology, Kharagpur in 2002.

Gautam Biswas, Professor
ISIS, Vanderbilt University
1025 16th Avenue
Nashville, TN, 37212, USA

email: gautam.biswas@vanderbilt.edu

Gautam Biswas received the PhD degree in computer science from Michigan State University, East Lansing. He is a Professor of Computer Science and Computer Engineering in the Department of Electrical Engineering and Computer Science, Vanderbilt University, Nashville, TN.

Kai Goebel, PhD
NASA Ames Research Center
Prognostics Center of Excellence
MS 269-1
Moffett Field, CA 94035, USA

email: kai.goebel@nasa.gov

Kai Goebel received the degree of Diplom-Ingenieur from the Technische Universitt Mnchen, Germany in 1990. He received the M.S. and Ph.D. from the University of California at Berkeley in 1993 and 1996, respectively. Dr. Goebel is a Senior Scientist at NASA Ames Research Center where he leads the Diagnostics and Prognostics groups in the Intelligent Systems division. In addition, he directs the Prognostics Center of Excellence and he is the technical lead for Prognostics and Decision Making of NASA's System-wide Safety and Assurance Technologies Program. He worked at General Electric's Corporate Research Center in Niskayuna, NY from 1997 to 2006 as a Senior Research Scientist. He has carried out applied research in the areas of artificial intelligence, soft computing, and information fusion. His research interest lies in advancing these techniques for real time monitoring, diagnostics, and prognostics. He holds 15 patents and has published more than 200 papers in the area of systems health management.